

## Vegetation–atmosphere interactions and their role in global warming during the latest Cretaceous

Garland R. Upchurch, Jr, Bette L. Otto-Bliesner and Christopher Scotese

*Phil. Trans. R. Soc. Lond. B* 1998 **353**, 97-112

doi: 10.1098/rstb.1998.0194

### Email alerting service

Receive free email alerts when new articles cite this article - sign up in the box at the top right-hand corner of the article or click [here](#)

To subscribe to *Phil. Trans. R. Soc. Lond. B* go to: <http://rstb.royalsocietypublishing.org/subscriptions>

# Vegetation–atmosphere interactions and their role in global warming during the latest Cretaceous

Garland R. Upchurch Jr<sup>1</sup>, Bette L. Otto-Bliesner<sup>2</sup> and Christopher Scotese<sup>3</sup>

<sup>1</sup> Department of Biology, Southwest Texas State University, San Marcos, TX 78666, USA (gu01@swt.edu)

<sup>2</sup> Climate Change Section, National Center for Atmospheric Research, PO Box 3000, Boulder, CO 80307-3000, USA (ottobli@ucar.edu)

<sup>3</sup> Department of Geological Sciences, University of Texas at Arlington, Arlington, TX 76019, USA

Forest vegetation has the ability to warm Recent climate by its effects on albedo and atmospheric water vapour, but the role of vegetation in warming climates of the geologic past is poorly understood. This study evaluates the role of forest vegetation in maintaining warm climates of the Late Cretaceous by (1) reconstructing global palaeovegetation for the latest Cretaceous (Maastrichtian); (2) modelling latest Cretaceous climate under unvegetated conditions and different distributions of palaeovegetation; and (3) comparing model output with a global database of palaeoclimatic indicators. Simulation of Maastrichtian climate with the land surface coded as bare soil produces high-latitude temperatures that are too cold to explain the documented palaeogeographic distribution of forest and woodland vegetation. In contrast, simulations that include forest vegetation at high latitudes show significantly warmer temperatures that are sufficient to explain the widespread geographic distribution of high-latitude deciduous forests. These warmer temperatures result from decreased albedo and feedbacks between the land surface and adjacent oceans. Prescribing a realistic distribution of palaeovegetation in model simulations produces the best agreement between simulated climate and the geologic record of palaeoclimatic indicators. Positive feedbacks between high-latitude forests, the atmosphere, and ocean contributed significantly to high-latitude warming during the latest Cretaceous, and imply that high-latitude forest vegetation was an important source of polar warmth during other warm periods of geologic history.

**Keywords:** palaeoclimate, global warming, vegetation, cretaceous, modelling

## 1. INTRODUCTION

A major unsolved problem in palaeoclimatology is understanding how warm polar temperatures can be maintained during periods of global warmth such as the Late Cretaceous. Two commonly proposed mechanisms for warming polar temperatures are increased atmospheric pCO<sub>2</sub> (Barron & Washington 1985) and increased heat transport by the world's oceans (Rind & Chandler 1991). Increased atmospheric pCO<sub>2</sub> warms global climate by absorbing outgoing longwave radiation and re-radiating it back to the surface. This warms surface temperatures at both equatorial and high latitudes because of the rapid global mixing of CO<sub>2</sub> in the atmosphere (Crowley 1991). Increased ocean heat transport, in contrast, removes heat from equatorial latitudes and transports it to high latitudes, which simultaneously cools the tropics and warms the poles (Crowley 1991). The most commonly proposed mechanism for warming high-latitude oceans is the generation of warm saline bottom water at low latitudes and upwelling of bottom water at high latitudes (Brass *et al.* 1982). Warming polar oceans through either mechanism creates positive feedbacks that further impact climate. These feedbacks include inhibition of sea-ice development, which increases absorption of solar radiation through

decreased ocean albedo, and increased concentrations of atmospheric water vapour at high latitudes, which enhance the greenhouse effect on a regional scale (but may also increase the cooling effect of clouds) (Rind & Chandler 1991). Both proposed mechanisms are supported by geochemical and oceanographic models (Bernier 1991, 1994; Brass *et al.* 1982) and by proxy indicators of atmospheric pCO<sub>2</sub> and ocean surface temperature (Andrews *et al.* 1995; Cerling 1991; Freeman & Hayes 1992; Huber *et al.* 1995).

Despite evidence for the operation of both mechanisms during periods of warm climate, model simulations that incorporate increased pCO<sub>2</sub> and increased ocean heat transport cannot fully recreate the warmth documented by biotic indicators for periods such as the Eocene and the Cretaceous. For the Early Eocene, the warmest interval during the Tertiary (Wolfe 1994; Wolfe & Upchurch 1987), atmospheric general circulation models (GCMs) simulate continental-interior temperatures that are too cold to explain the geographic distribution of cold-sensitive plants such as palms and cycads (Sloan & Barron 1992; Wing & Greenwood 1993). For the Mid-Cretaceous, GCMs create winter surface temperatures that are too cold in continental interiors to explain the distribution of cold-sensitive fossil plants (Barron &

ington 1982). The problem with freezing continental interiors can persist in model simulations that greatly reduce ocean transport (e.g. Schneider *et al.* 1985; Sloan & Arron 1990), which indicates that a combination of mechanisms may be needed to explain the warmth of periods such as the Eocene and the Cretaceous.

One mechanism neglected in discussions of warm-temperate dynamics is the role of the land surface in maintaining high-latitude warmth, and in particular the role of vegetation. Vegetation plays in regulating fluxes of energy, water vapour, and momentum between the land surface and the atmosphere (Dickinson *et al.* 1986; Sellers *et al.* 1986). Vegetation absorbs a significant fraction of incoming solar radiation, which decreases surface albedo relative to bare soil. Vegetation transpires significant quantities of water vapour from stomata during the uptake of carbon dioxide for photosynthesis, which increases the flux of latent heat from the land surface. The extensive surface area of vegetation created by leaves and stems increases aerodynamic drag of the land surface (surface roughness), which increases the rate of transfer of mass and energy between the land surface and the atmosphere. A good example of vegetation's importance in regulating climate occurs in modern boreal regions, where the presence of forest vegetation controls the position of the winter front, increases the length of the growing season, causes early snow melt relative to tundra (e.g. Brown 1966; Foley *et al.* 1994; Pielke & Vidale 1995). Increasing the areal extent of high-latitude forests has temperature effects comparable to a doubling of greenhouse gases or orbital forcing (Bonan *et al.* 1992; Foley *et al.* 1994). This implies that vegetation played an important role in maintaining warm polar climates during periods such as the Late Cretaceous, because high-latitude forests occupied extensive regions that today are occupied by tundra or glacial ice (Creber & Chaloner 1991; Horrell 1991; Spicer & Parrish 1990; Wolfe & Upchurch 1987).

Our study explores the importance of high-latitude forests in maintaining polar warmth during the Late Cretaceous and feedbacks between the land, atmosphere, and ocean. We do this through a combination of numerical climate modelling and comparison of model results with a global data base of climatic indicators. We examine the importance of vegetation in the climate system by simulating latest Cretaceous (Maastrichtian) climate under different types of vegetation cover, then determine the extent to which modelled climates resemble modern climates. We focus on the Maastrichtian climate because of its importance for understanding extinctions at the Cretaceous–Tertiary boundary. However, many of our conclusions can be extrapolated to the Mid- and Early Cretaceous because these periods also were characterized by areally extensive polar forests (Spicer & Parrish 1990; Wolfe & Upchurch 1987). Here we focus on land–atmosphere–ocean interactions to demonstrate the interconnectedness of the biosphere, atmosphere, and ocean.

#### MODEL DESCRIPTION

The model used in this study is the National Center for Atmospheric Research (NCAR) GENESIS Global

Climate Model, v. 1.02, which consists of submodels for the atmosphere, ocean, and land surface (Thompson & Pollard 1995*a,b*). The atmosphere submodel is derived from the NCAR Community Climate Model (CCM1), and is described by equations of fluid motion, thermodynamics, and mass continuity along with representations of radiative and convective processes, cloudiness, precipitation, and the orographic influence of terrain. The modified CCM1 code incorporates new physics for solar radiation, water vapour transport, convection, boundary layer mixing, and clouds. Horizontal resolution is R15 for the atmosphere (approximately 4.5° latitude by 7.5° longitude) and 2° by 2° for the land surface. The atmosphere is subdivided vertically into 12 levels.

The ocean submodel of GENESIS contains a 50 m deep mixed-layer ocean coupled to a thermodynamic sea-ice model, which crudely captures the seasonal heat capacity of the ocean mixed layer but ignores salinity, upwelling, and energy exchange with deeper layers. Poleward ocean heat transport is parameterized as diffusion using the '0.5 × OCNFLX' case of Covey & Thompson (1989). A six-layer sea-ice model, patterned after Semter (1976), predicts local changes in sea ice thickness through melting of the upper layer and freezing or melting of the bottom surface.

The land surface submodel of GENESIS (Pollard & Thompson 1995) incorporates a land surface transfer component (LSX) to account for the physical effects of vegetation, a six-layer soil component, and a three-layer thermodynamic snow component. Soils are categorized by colour and texture. Vegetation is represented by two layers: an upper layer of trees or shrubs, and a lower layer of grass or bare soil. Vegetation prescription includes type, leaf area index (LAI), fractional coverage of plants, canopy height, solar transmittance/reflectance, and stomatal resistance. The physical attributes of the vegetation are fixed: vegetation can respond to climate physiologically, but it cannot respond by changing LAI, fractional cover, or other structural attributes (Pollard & Thompson 1995).

The physical and biological realism in LSX and comparable models (e.g. the biosphere–atmosphere transfer scheme (BATS) of Dickinson *et al.* (1986)) represent a major improvement over the bucket hydrology and fixed surface albedoes of earlier GCMs. However, LSX makes certain simplifying assumptions about vegetation that are biologically unrealistic. For example, LAI, fractional coverage, and other attributes of a given vegetation type are fixed over its full geographic range and do not vary in response to regional differences in temperature, precipitation, or soil nutrient status. Minimum stomatal resistance is fixed at a predetermined value, rather than calculated as a function of atmospheric pCO<sub>2</sub>. Many potentially interesting interactions between vegetation and climate cannot be investigated, including reciprocal and interactive changes over time between climate, LAI, and life-form abundance. However, LSX and similar models provide reasonable simulations of land surface albedo, surface roughness, and energy fluxes for the present day (e.g. Sellers & Dorman 1987), which enable us to investigate first-order climatic effects of vegetation for periods of the geologic past.

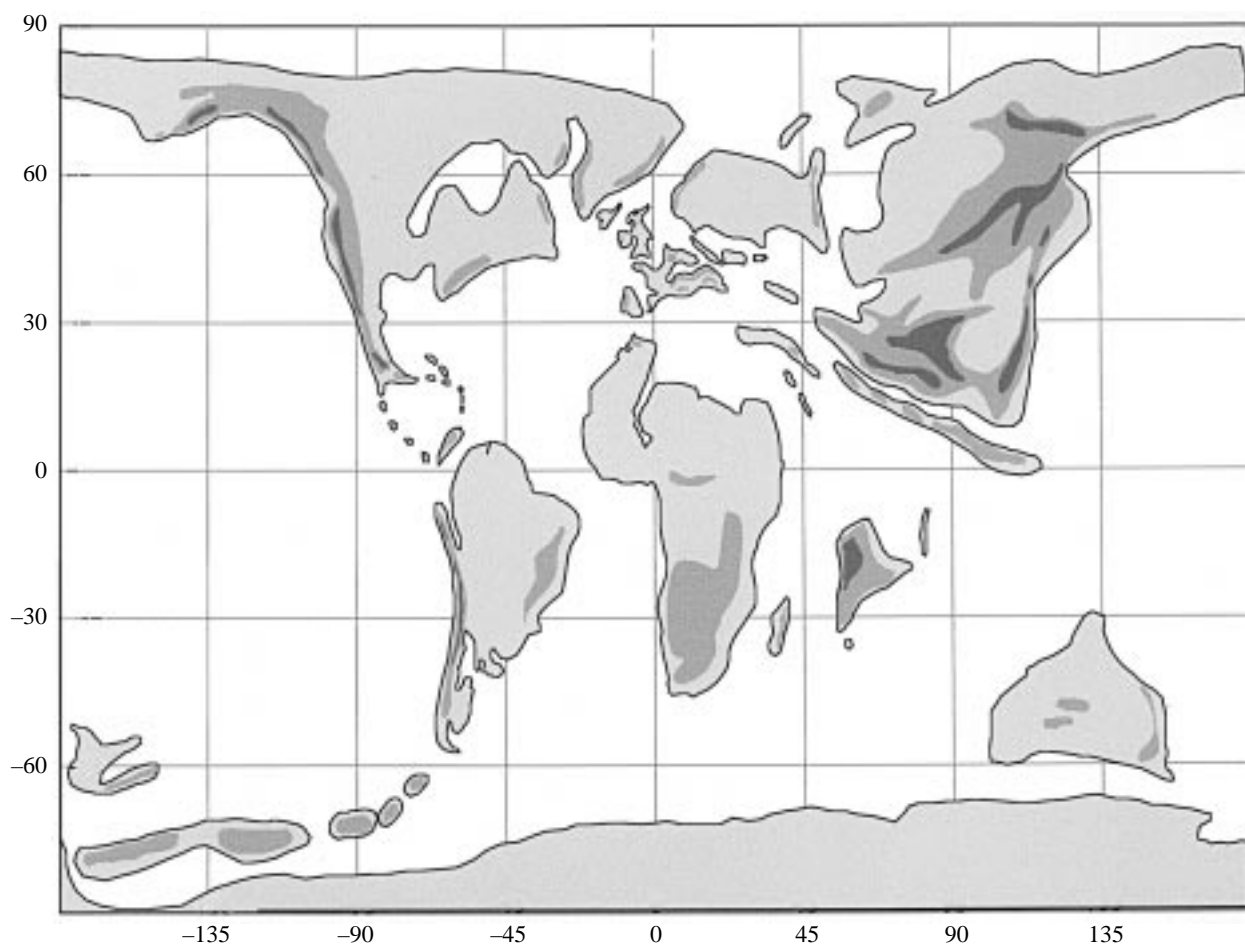


Figure 1. Palaeogeography for the latest Cretaceous (latest Maastrichtian). Lightly stippled areas designate lowlands, medium and dark stippled areas designate highlands.

### 3. SIMULATIONS

#### (a) *Boundary conditions*

Prescribed boundary conditions include  $p\text{CO}_2$ , land-sea distribution, elevation, and solar luminosity. Atmospheric  $p\text{CO}_2$  is set at twice pre-industrial levels (580 ppm), a level slightly higher than the 'best estimate' of geochemical models (Berner 1994) and significantly lower than the best estimates of isotopic proxies (Andrews *et al.* 1995; Freeman & Hayes 1992). We set  $p\text{CO}_2$  at this conservative figure to keep the high latitudes relatively cool. This allowed us to evaluate more clearly the temperature effects of high-latitude forests with our database of global palaeoclimatic indicators, which maps the position of a few important isotherms instead of providing estimates of mean annual temperature for numerous data sites. Palaeogeography (figure 1) is drawn for the latest Cretaceous (latest Maastrichtian), a time of regression for both the Western Interior seaway of North America and the Trans-Saharan seaway of Africa. Palaeoelevations are set to 250 m for lowlands and 1000 and 2000 m for uplands, a compromise between two palaeogeographic formulas (Hay 1984; Ziegler *et al.* 1985). Solar insolation conforms to present-day solar orbital configuration with the solar constant adjusted to 0.664% less than at present (Crowley & Baum 1992; Endal 1981).

#### (b) *Model experiments*

For our larger study, we conducted five simulations to explore the sensitivity of Late Cretaceous palaeoclimate to major changes in palaeovegetation. BARESOIL supplies benchmark statistics for a world with no vegetation, and is the boundary condition used in many earlier simulations of Cretaceous climate. Soil texture and colour are set to intermediate values in the range given by BATS, with an average snow-free land albedo of 15% (Dickinson *et al.* 1986). EVERGREEN TREE provides maximum LAI and fractional cover to explore the range of climatic effects exerted by areally widespread forests. Broad-leaved evergreen trees (tropical rainforest) are prescribed over all land surfaces at a fractional coverage of 98%; surface albedo over high-latitude land varies only slightly from 12% in summer to 18% in winter. An additional simulation, EVERGREEN TREE-OHT, adds tripled ocean heat transport to the effects of evergreen forest vegetation, to explore the sensitivity of a fully vegetated Earth to warm Cretaceous polar oceans.

The final two simulations are based on best estimates of vegetation (table 1, figure 1 and below). BESTGUESS uses the best estimate of vegetation based on a variety of lithologic and palaeontologic indicators (figure 2). An individual  $2^\circ \times 2^\circ$  land surface grid was coded for a particular vegetation type based on a palaeontologic or

Table 1. *Latest Cretaceous vegetation types and their defining features\**

Biophysical parameters estimated for fossil vegetation represent unweighted averages of values listed for the closest SiB biomes (Dorman & Sellers 1989). The exception is our biome 3, which is weighted, as follows, to increase the importance of broadleaf evergreens: SiB biome (1+1+2)/3. Fractional cover for our biome 3 is based on the weighted average multiplied by 0.8. This method used the more open canopy conditions inferred from foliar physiognomy and *in situ* megafossil assemblages preserved in volcanic ash (Wing *et al.* 1993; Wolfe & Upchurch 1987).

Biome number	Biome name	Recognition criteria	Closest SiB biomes	Canopy height	Areal cover	Stomatal resistance (s m <sup>-1</sup> )
	tropical rainforest	equatorial latitude plus one or more of the following: coals, megaflores with large leaves and drip tips, tree ferns	1	35 m	0.98	154
	tropical semi-deciduous forest/woodland	tropical latitudes plus the absence of coals and evaporites; calcretes may be present	1, 6	26 m	0.64	160
	subtropical broad-leaved evergreen forest and woodland	middle latitudes; angiosperm dominance in megaflores and palynoflores plus megaflores with small evergreen leaves and few or no drip tips, presence of palms or gingers, fossil wood without growth rings, thick angiosperm leaf cuticles, cold-sensitive fungal taxa	1, 2	30 m	0.72	163
	desert and semi-desert	low and middle latitudes; evaporites, calcretes, or evidence for treeless conditions	9	0.5 m	0.10	855
	temperate evergreen coniferous and broad-leaved forest	high middle latitudes; high relative abundance and diversity of conifers in palynoflores and cuticle assemblages plus numerous probable evergreens in palynoflores and cuticle assemblages, cold-sensitive fungal taxa	4	17 m	0.75	233
	polar deciduous forest	high latitudes; megaflores without tundra leaf form and dominated by deciduous angiosperm and conifer leaves, fossil tree stumps with annual growth rings, at least 2–3 tree genera in pollen record	2, 5	17 m	0.62	206
	bare soil (used to code cold deserts)	calcretes present, associated with extremely low-diversity palynoflores	11	0.05 m	0.00	100

Biome numbers correspond to those used in figure 1. Our biome 6, tropical savannah, is not mentioned in the table because grasses do not appear in the fossil record until the Tertiary. SiB refers to the Simple Biosphere Model (Dorman & Sellers 1989; Sellers *et al.* 1986). SiB biomes are as follows: 1, broadleaf evergreen trees; 2, broadleaf deciduous trees; 4, needleleaf evergreen trees; 5, needleleaf deciduous trees; 6, broadleaf trees with ground cover (tropical savannah, only the upper story used); 9, broadleaf shrubs with bare soil; 11, no vegetation, bare soil.

Biome 3 is a paleogeographic indicator. For regions where geologic data were not available, output from EVERGREEN TREE-OHT was used to describe vegetation because the output of this simulation best-fit the record of palaeoclimatic indicators. While the method of interpolation may seem somewhat circular, we consider it superior to intuition or guesswork. Physical and physiological parameters were assigned to each fossil vegetation type by comparing each with the most similar extant vegetation type and using the parameters for extant vegetation listed by Dorman & Sellers (1989). When a fossil biome had no extant counterpart, averages of the one or three most similar extant biomes were used. No vegetation type was recognized for palaeovegetation in the understorey layer. LSX only recognizes grass for the understorey. Grasses do not appear in the fossil record until the Palaeocene (Crepet & Feldman 1991; Muller 1981), while

grassland vegetation does not appear in the fossil record until the Miocene–Pliocene (Cerling *et al.* 1994).

BESTGUESS-RS2 is similar to BESTGUESS but it doubles the resistance of leaf stomata to diffusion of carbon dioxide and water vapour. We applied this doubling to all vegetation types to provide a parallel simulation to that of Pollard & Thompson (1995), who simulated modern climates under doubled stomatal resistance to approximate one aspect of future vegetational response to doubled pCO<sub>2</sub>. In both studies, stomatal resistance was doubled in the absence of other vegetational changes to isolate the climatic effect of increased stomatal resistance from other changes, such as increased LAI resulting from increased productivity under elevated pCO<sub>2</sub>.

Here we expand on the results presented in Otto-Bliesner & Upchurch (1997). We focus on the BARESOIL

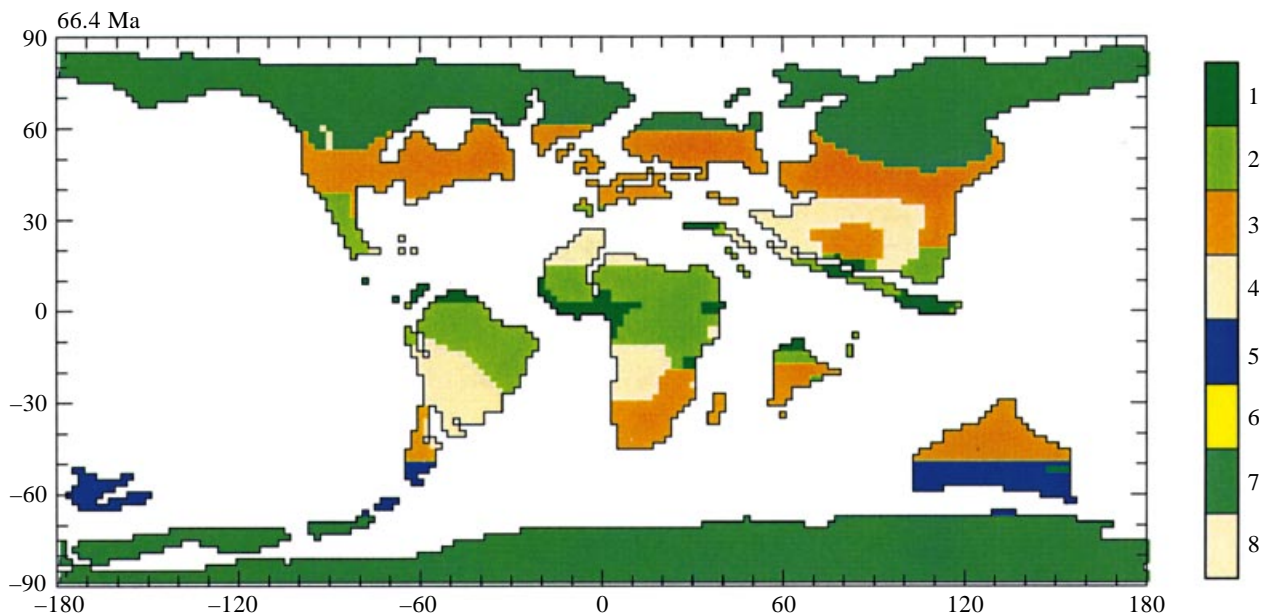


Figure 2. BESTGUESS estimate of Maastrichtian vegetation. Lithologic and palaeontologic indicators were used as primary data, and output from the EVERGREEN TREE-OHT simulation (not reported in this paper) was used to code regions between data points. Vegetation categories and criteria for recognition are explained in table 1. Polar deciduous forest is inferred for Antarctica based on the prevalence of such vegetation at high latitudes in the Northern Hemisphere. Bare soil is used to code for cold deserts with extremely low floristic diversity that are located near the Laramide Front in the Western Interior of North America. Subtropical woodlands have indicators of above-freezing winters such as palms. No Maastrichtian equivalent of Mediterranean woodlands and chaparral is used in BESTGUESS simulations, although some model simulations predict the occurrence of such vegetation in restricted regions. Legend: 1, tropical rainforest; 2, tropical semi-deciduous forest; 3, subtropical broad-leaved evergreen forest and woodland; 4, desert and semi-desert; 5, temperate evergreen broad-leaved and coniferous forest; 6, tropical savannah (not used here); 7, polar deciduous forest; 8, bare soil.

and BESTGUESS simulations to illustrate the important effects of palaeovegetation on global and regional palaeoclimate. A fuller description of other simulations, including the statistical significance of differences between simulations, is provided elsewhere (Upchurch *et al.* 1998).

### (c) *Palaeovegetation and palaeoclimatic data*

All simulations were compared with a global data base of palaeovegetation indicators to evaluate the success of each simulation in reproducing the Maastrichtian climate. Palaeobotanical indicators of vegetation and climate include the physiognomy of leaf megafossils (Wolfe & Upchurch 1987), life form as inferred from leaf megafossils and fossil woods (Upchurch & Wolfe 1993), the physiognomy of dispersed leaf cuticles (Upchurch 1995), and the anatomy of fossil woods (e.g. the presence or absence of growth rings) (Creber & Chaloner 1985). Palynologic data were used selectively because of problems associating many palynomorphs with individual life forms. Palynologic indicators employed in this study included (1) the spores of *Sphagnum* moss, which were used as an indicator of wet soils; (2) the spores of aquatic ferns, which were used as indicators of ponded water; (3) structurally complex spores and pollen of tree ferns and palms, which were used as indicators of above-freezing conditions; and (4) the presence of at least two or three genera of pollen whose extant relatives comprise trees, which were used as evidence for forest vegetation.

Global palaeobotanical data were particularly useful in reconstructing two isotherms that delimit vegetation

boundaries: (1) a warm-month mean of 10 °C, which delimits the boundary between forest and tundra vegetation (Köppen 1936; Wolfe 1979), and (2) a cold-month mean of 1 °C, which is the lowest monthly mean temperature that delimits the boundary between vegetation with freeze-sensitive life forms and vegetation dominated by freeze-tolerant life forms (Wolfe 1979). Warm-month means higher than 10 °C were documented by indicators of the tree growth habit, including fossil woods greater than 10 cm in diameter, leaf megafossil assemblages with physiognomy indicative of forest (rather than tundra) vegetation (Bailey & Sinnott 1916), and the presence of at least 2–3 genera of fossil pollen whose living relatives comprise trees. Cold-month means of greater than 1 °C were documented by fossil organisms whose life form and physiology make them susceptible to hard freezes. These organisms include (i) fossil palms, tree ferns, and evergreen cycads, which have the freeze-sensitive rosette tree or rosette shrub growth habit (Box 1981); (ii) epiphyllous fungi (Loculoascomycetes belonging to the genus *Trichopeltinites*), which are sensitive to below-freezing temperatures (Dilcher 1965); and (iii) woods that have no growth rings, which indicate poorly developed dormancy mechanisms (Creber & Chaloner 1985).

The location of the forest–tundra boundary and the line of hard freezing were emphasized in model evaluation because these vegetation boundaries are best predicted by temperature, rather than moisture availability (Köppen 1936; Wolfe 1979). This is because vegetation boundaries during the Late Cretaceous probably were delimited by different precipitation values than those of the Recent due

enhanced water-use efficiency of Late Cretaceous plants or elevated pCO<sub>2</sub>. We make this uniformitarian assumption with the caveats that (1) the effect of elevated CO<sub>2</sub> on physiological processes at low temperatures is not well understood; and (2) the temperature parameters delimited vegetation during the Late Cretaceous may have been somewhat different from those of today because of elevated pCO<sub>2</sub> and the evolutionary status of Cretaceous floras.

Plant types supplemented palaeobotanical data and are particularly important in the tropics and in regions with dry climates. Coals served as indicators of wet soils and abundant rainfall (Ziegler *et al.* 1987), and in equatorial regions served as an indicator of tropical rainforest (Went 1991). Evaporites and calcretes served as indicators of seasonal or annual moisture deficit (Ziegler *et al.* 1992), with evaporites tentatively associated with arid conditions and calcretes associated with seasonally dry conditions. Approximately 500 individual citations of plant and sediment types were used in reconstructing late Maastrichtian global vegetation and climate. The most important of these citations are plotted in maps in this paper and are provided as supplementary information in Otto-Bliesner & Upchurch (1997) and as appendix in Upchurch *et al.* (1998).

## RESULTS OF SIMULATIONS

### BARESOIL and BESTGUESS surface temperatures (figures 3–7; table 2)

In the BARESOIL simulation, January surface air temperatures (temperatures simulated at 2 m above the surface) are warmer than for the present day, but still are generally cold at high latitudes in the Northern Hemisphere. The freezing isotherm extends equatorially to 45° over North America and 38° N over eastern Asia. The northern Interior Seaway of North America is almost completely frozen, and temperatures as low as –34 °C are modelled over the Asian interior. Mean cold-month surface temperatures for most of Europe are below freezing. Surface temperatures in Antarctica and Australia are above freezing during the austral summer. Antarctica has no permanent ice cover because all snow cover melts during the summer months. Mean surface temperatures are only a few degrees below zero over Antarctica, and sea-ice covers the continent. Subfreezing temperatures also occur over the southern portions of Australia.

In both hemispheres, cold winter temperatures at high latitudes result from extensive snow cover and its high albedo. Mean land surface albedo ranges from 0.39–0.65, with values as high as 0.84 during the winter. Mean annual temperatures range from 25–35 °C. Global mean surface temperature in the BARESOIL simulation is 15.5 °C, one degree warmer than what the model predicts for the present day (14.8 °C).

In the late Maastrichtian land surface in BESTGUESS is simulated with vegetation types that vary from tropical rainforest to cold desert (figure 2). Tropical rainforests are predicted in areal distribution relative to the Recent and are found in Colombia, central Africa, Somalia, and southern Asia. Deserts and semi-deserts occur over large areas in central Asia, South China, northern Africa, southern Africa, and central South America. Tropical

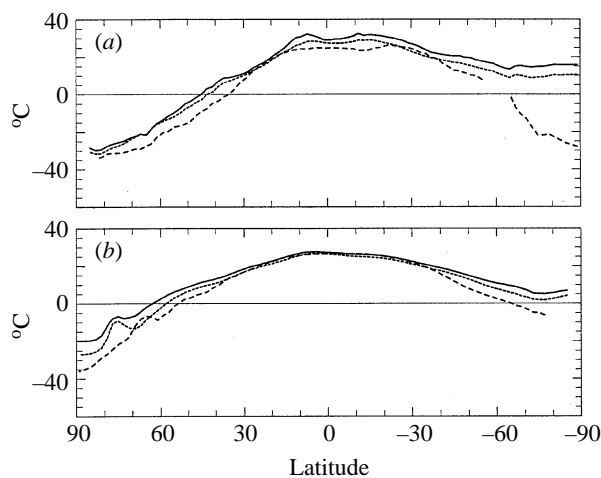


Figure 3. Zonally averaged surface temperature (at a height of 2 m) simulated by the GENESIS climate model in January for (a) land and (b) ocean. The solid line (top line) is the BESTGUESS simulation and the dotted line (middle line) is the BARESOIL simulation. The dashed line is the present-day control simulation.

deciduous forests are inferred to have occupied most regions between tropical rainforest and desert vegetation.

Mid- and high-latitude vegetation types show strong poleward displacement relative to their Recent counterparts. Warm-temperate to subtropical evergreen forests and woodlands with cold-sensitive plants such as palms occur over most mid-latitude regions as far poleward as 50° latitude. Poleward of 50° N in the Northern Hemisphere, these evergreen forests/woodlands are replaced by polar deciduous forest, which occupies extensive regions of Canada, Alaska, and Siberia. Poleward of 50° S in the Southern Hemisphere, these evergreen forests are replaced by temperate evergreen coniferous and broad-leaved forests. These forests, which occur in northern Australia, New Zealand, and the Antarctic Peninsula, are similar in their inferred physiognomy and floristic composition to Recent forests of New Zealand. Deciduous forests are inferred to have been present on mainland Antarctica, but direct evidence for their existence is lacking because relevant geologic strata are covered with glacial ice.

In the BESTGUESS simulation, surface temperatures at high latitudes are warmer, most notably during the summer. January land surface temperatures are up to 2–4 °C warmer over high northern latitudes (e.g. Siberia, Alaska), and the average position of the 1 °C isotherm shifts somewhat poleward (figure 11). Subfreezing temperatures still exist over the northern interior regions of North America and Asia. January temperatures over Siberia are as much as 8 °C cooler in BESTGUESS relative to BARESOIL; the reason for this cooling requires further study. July surface temperatures are up to 8 °C warmer over high northern latitudes. The Antarctic interior is 4–8 °C cooler in the BESTGUESS simulation, although this cooling of the Antarctic interior is generally not statistically significant. Mean tropical surface temperature warms by 1.5 °C, with regions of semi-deciduous forest in Africa and South America warming by as much as 4 °C. This warming results from a decrease in albedo and a corresponding increase in absorbed solar radiation. Global mean surface temperature warms by

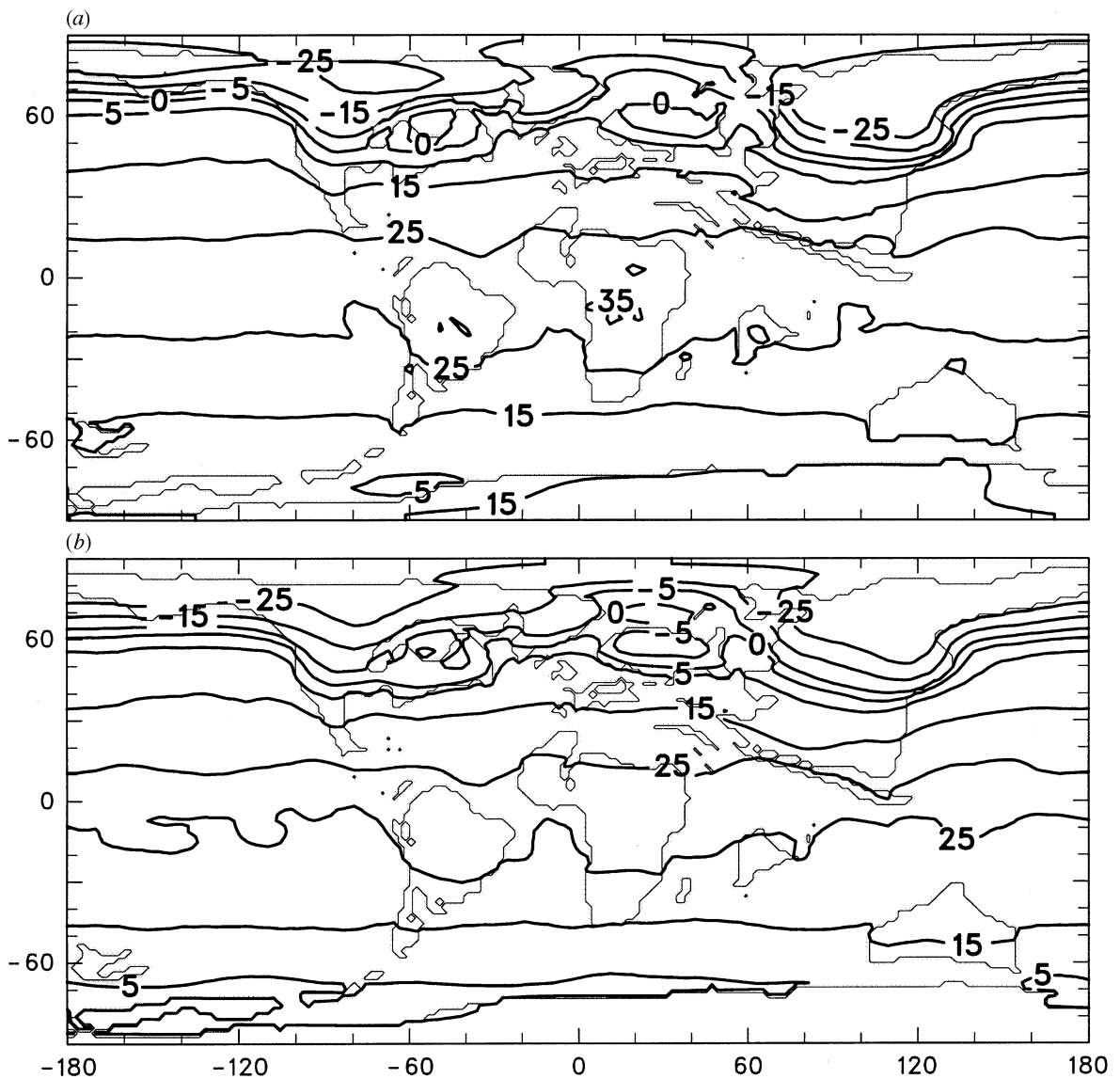


Figure 4. January mean surface air temperature ( $^{\circ}\text{C}$ ) for (a) BESTGUESS and (b) BARESOIL simulations.

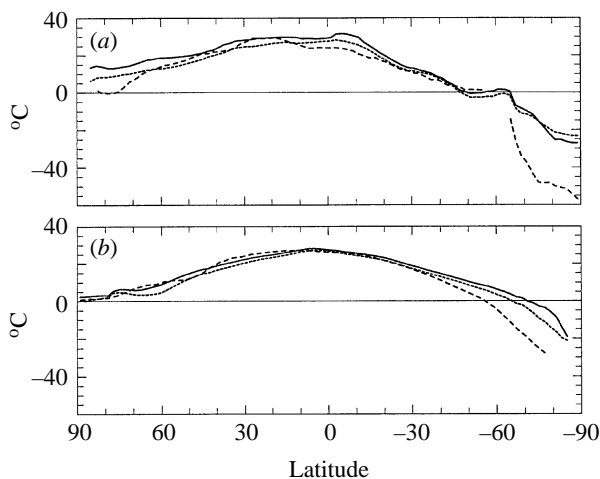


Figure 5. Zonally averaged surface temperatures ( $^{\circ}\text{C}$ ) in July for (a) land and (b) ocean. The solid line is the BESTGUESS simulation and the dotted line is the BARESOIL simulation. The dashed line is the present-day control simulation.

$2.2^{\circ}\text{C}$  to a value of  $18.0^{\circ}\text{C}$  in a late Maastrichtian world covered with realistic vegetation.

Terrestrial vegetation causes significant changes in ocean temperature. Surface temperatures over tropical and mid-latitude oceans warm by up to  $4^{\circ}\text{C}$  in the BESTGUESS simulation because energy is transferred from land to the adjacent ocean. High-latitude oceans warm by as much as  $12^{\circ}\text{C}$ , resulting in substantially lower fractional coverage of sea-ice in BESTGUESS relative to BARESOIL (0.06 versus 0.17 in the Southern Hemisphere and 0.23 versus 0.38 in the Northern Hemisphere). The average winter sea-ice position moves poleward from  $60^{\circ}\text{N}$  to  $65^{\circ}\text{N}$  in January and from  $65^{\circ}\text{S}$  to  $73^{\circ}\text{S}$  in July.

(b) *The surface energy budget at high latitudes (figures 8–9)*

The presence of forest vegetation at high latitudes initiates feedbacks between albedo, surface temperature, and snow and ice cover that result in a much warmer climatic regime. This is dramatically illustrated by a comparison of the BARESOIL and BESTGUESS simulations for regions



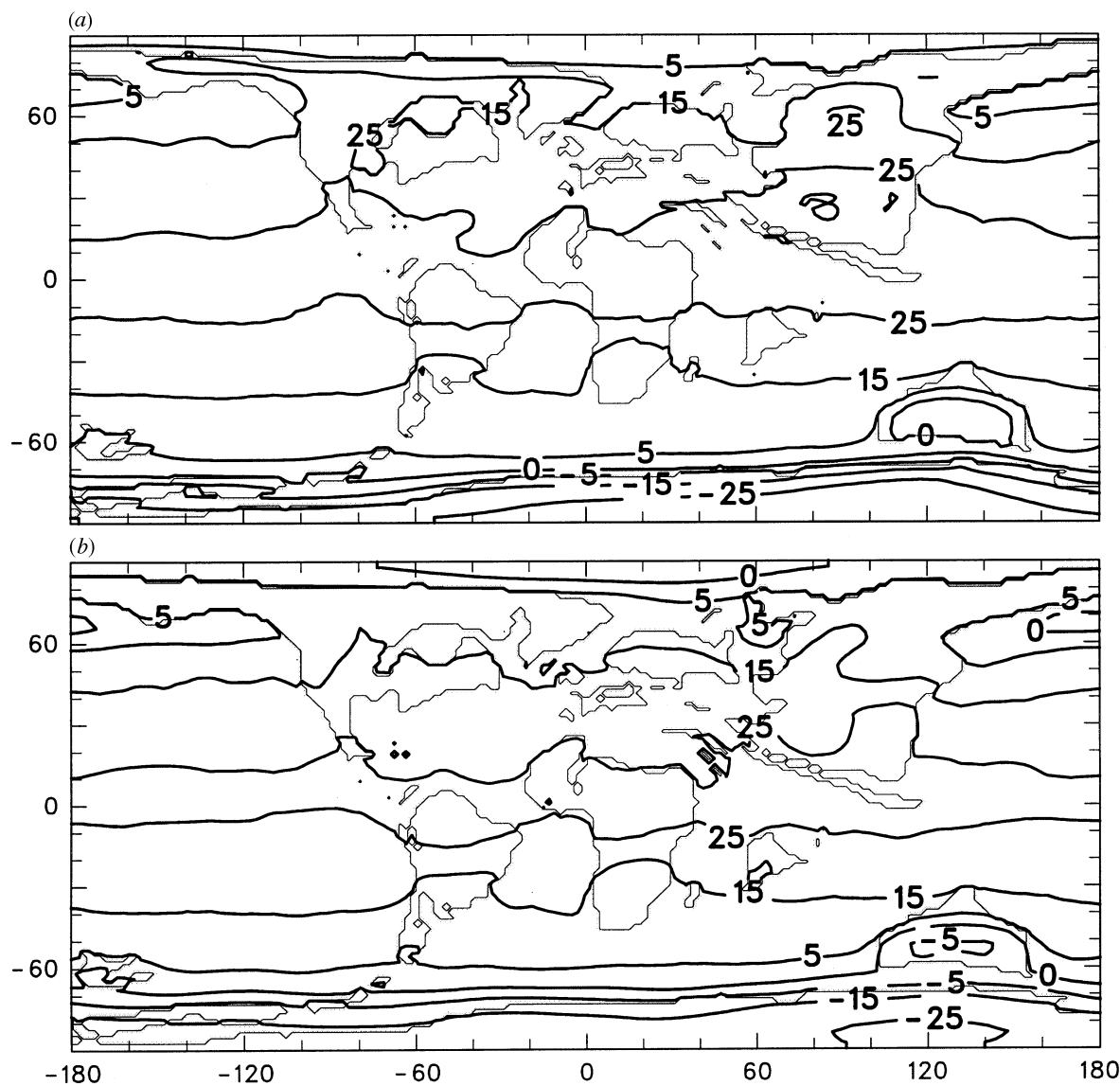


Figure 6. July mean surface air temperature ( $^{\circ}\text{C}$ ) for (a) BESTGUESS and (b) BARESOIL simulations.

$10^{\circ}$  N. Vegetation reduces land surface albedo year-round, especially from January through June when insolar radiation is increasing at high northern latitudes. From late winter to early spring, the trees partially mask the snow on the ground and absorb more incoming radiation because of their lower albedoes. In spring to early summer, surface albedoes are lower, forest vegetation occurring due to earlier spring melting of snow cover and the presence of leaves on the ground. Fractional snow cover for May is only 50% in the BESTGUESS simulation, but remains greater than 80% in the BARESOIL simulation, even for June. The net effect of the lower surface albedoes is to allow more solar radiation to be absorbed at the land surface in the BESTGUESS simulation (78% more than in the BARESOIL simulation for April to June).

At high northern latitudes, changes in the other components of the surface energy budget moderate the response of the vegetated land surface to changes in absorbed solar radiation. In late winter to early spring, increases in absorbed solar radiation in BESTGUESS

are largely offset by (1) increased surface cooling due to enhanced longwave radiation, and (2) decreased transfer of sensible heat from the atmosphere to the land surface. From April to June, however, vegetation increases absorbed solar radiation by an average of  $65 \text{ W m}^{-2}$ , an increase that is only partially offset by increased energy fluxes from the land surface. The result is an average net energy gain of  $6 \text{ W m}^{-2}$ , which produces warmer surface temperatures and faster snow melt. Average land surface temperature from  $60\text{--}90^{\circ}$  N in BESTGUESS rises above freezing by mid-April and above  $10^{\circ}\text{C}$  by late May, and remains above freezing until late October. In contrast, average land surface temperature from  $60\text{--}90^{\circ}$  N in BARESOIL rises above freezing in early May, reaches a maximum of  $10^{\circ}\text{C}$  in early July, and falls below freezing by late September.

A portion of the extra energy absorbed by vegetated land areas is advected to nearby high-latitude oceans, which initiates feedbacks between surface temperature, ice cover, surface albedo, and the surface energy budget. In BESTGUESS, the average ocean temperature from

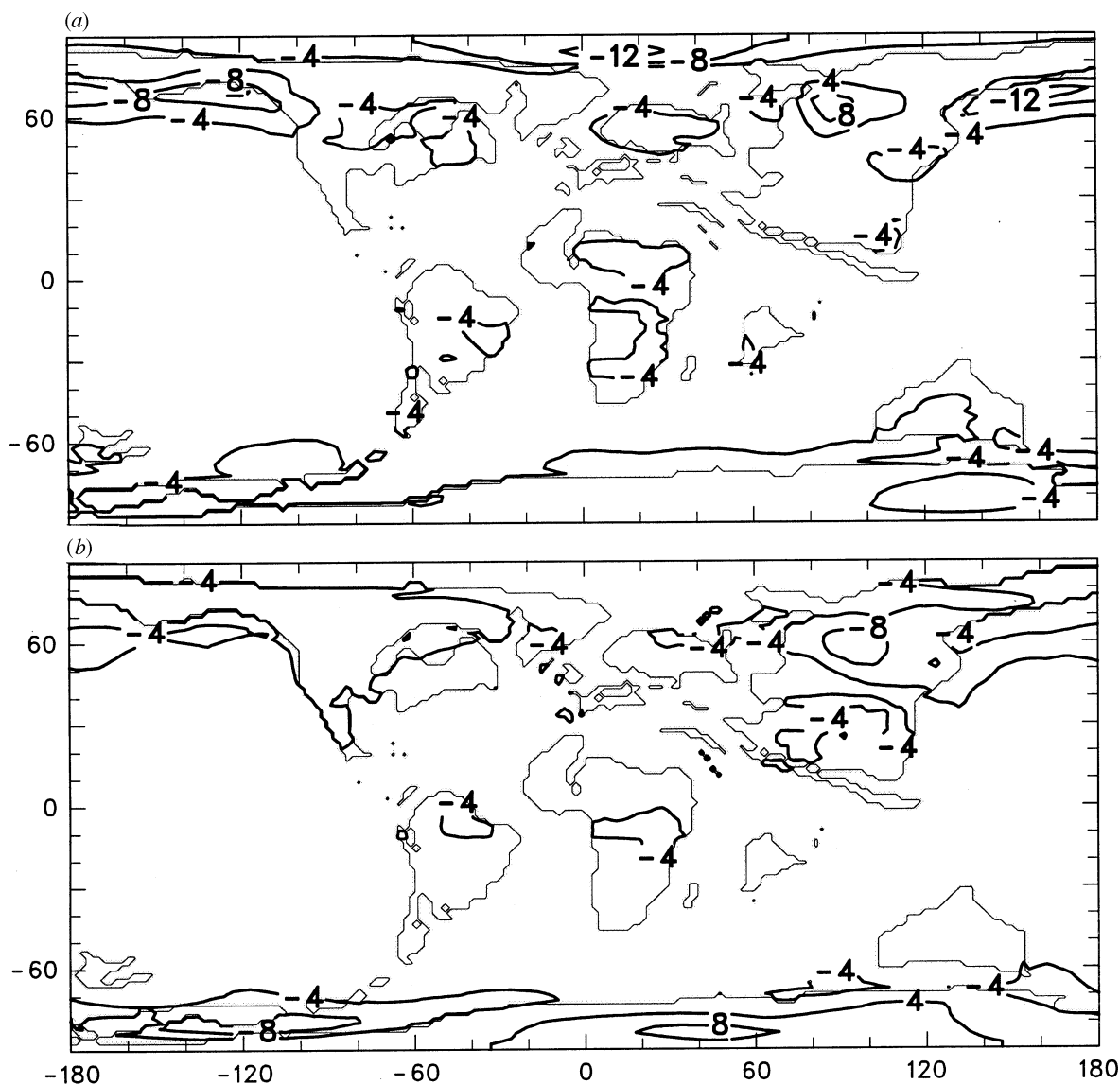


Figure 7. Changes in surface air temperature ( $^{\circ}\text{C}$ ) for (a) January BARESOIL minus BESTGUESS, and (b) July BARESOIL minus BESTGUESS. Negative values mean that the BESTGUESS simulation was warmer than the BARESOIL simulation, while positive values indicate that the BESTGUESS simulation was colder.

60–90° N falls below freezing ( $-2^{\circ}\text{C}$ ) for only four months, rather than six months as in BARESOIL. Average fractional coverage of sea-ice in BESTGUESS exceeds 50% only from mid-February to early May. This causes large decreases in ocean surface albedo relative to BARESOIL from April to June and large increases in absorbed radiation. The result of these changes is a net warming of oceans, which inhibits the development of sea-ice during the subsequent autumn and winter. Ocean warming, in turn, ameliorates winter temperatures on land, especially for regions immediately adjacent to the coast (figure 7a,b).

(c) **Regional variation in climate (figure 10)**

The Köppen system correlates Recent vegetation with climate using monthly mean temperature and precipitation. For the Late Cretaceous, when elevated  $\text{pCO}_2$  may have altered the climatic tolerances of individual life forms and vegetation types, the Köppen system provides a simple and convenient means of visualizing regional climatic variation. The GENESIS climate model accurately reproduces the

modern-day distribution of Köppen climate types, especially the boundary between warm-temperate (C), cool-temperate (D), and tundra (E) climates. Regional features, such as rain-shadow deserts and the Indian monsoon, are inadequately simulated because of model-smoothing of mountain topography. This deficiency is not critical for evaluating latitudinal variation in climate. Our comparison here is based on a modified Köppen system where the boundary between warm-temperate (C) and cool-temperate (D) corresponds to a cold-month mean of  $1^{\circ}\text{C}$  (Wolfe 1979), rather than  $-8^{\circ}\text{C}$  (Köppen 1936), and the boundary between subtropical (Cfa) climates with angiosperm-dominated vegetation and marine (Cfb, Cfc) climates with conifer-dominated vegetation is set at a warm-month mean of  $20^{\circ}\text{C}$ , based on the temperature parameters of Recent forests in east Asia (Wolfe 1979).

The BARESOIL and BESTGUESS simulations contrast markedly with each other and with the present day. In BARESOIL, tropical rainforest (Af) is restricted to small regions in Colombia, west Africa, India, and south-east Asia. Marine climates (Cfb, Cfc) with cool

Table 2. Simulated mean annual climate statistics

ranges for years 14–20 of the BARESOIL and BESTGUESS simulations. All Cretaceous simulations use CO<sub>2</sub> of 580 ppm, or twice the pre-industrial value. Temperature values are for 2 m above the land or ocean surface. The Bowen ratio is the ratio of sensible to latent heat

Parameter	BARESOIL	BESTGUESS
Annual mean surface temperature (°C)		
Global	15.8	18.0
60–90° N	−5.5	−1.4
30° N–15° S	26.1	27.6
60–90° S	−0.8	2.6
60–90° N		
Annual cloudiness	0.65	0.63
Surface albedo	0.40	0.19
Surface absorbed solar radiation (W m <sup>−2</sup> )	72.1	93.1
Outgoing surface infrared radiation (W m <sup>−2</sup> )	33.1	41.1
Surface sensible heat flux (W m <sup>−2</sup> )	5.8	12.8
Surface latent heat flux (W m <sup>−2</sup> )	32.6	39.2
Bowen ratio	0.16	0.36
Surface temperature (°C)	−7.5	−3.3
Fractional snowcover	0.62	0.52
60–90° S		
Annual cloudiness	0.70	0.69
Surface albedo	0.39	0.18
Surface absorbed solar radiation (W m <sup>−2</sup> )	64.8	84.0
Outgoing surface infrared radiation (W m <sup>−2</sup> )	30.5	37.7
Surface sensible heat flux (W m <sup>−2</sup> )	4.7	9.4
Surface latent heat flux (W m <sup>−2</sup> )	29.7	37.2
Bowen ratio	0.14	0.26
Surface temperature (°C)	−5.8	−2.5
Fractional snow cover	0.63	0.52
60–90° N		
Surface temperature (°C)	−3.3	0.7
Fraction	0.38	0.23
60–90° S		
Surface temperature (°C)	1.8	5.3
Fraction	0.17	0.06
15° S–15° N		
Surface temperature (°C)	25.8	26.9

temperatures, mild winters, and evergreen forests cover southern Africa, southern South America, and the northern margins of Europe and North America. Cool-temperate (D) climates with below-freezing winters and deciduous or boreal forests cover much of North America, Asia, and Antarctica. Tundra (ET) is predicted for much of Asia and coastal regions of North America and Antarctica.

BESTGUESS, tropical rainforest climate increases areal extent in South America, south-east Asia, India, east Africa, and replaces ‘savannah-type’ (Aw)

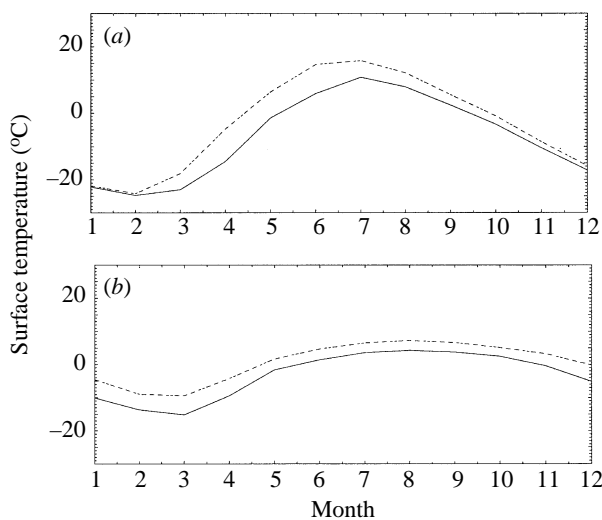


Figure 8. Annual cycle of surface temperature for BESTGUESS (dashed lines) and BARESOIL (solid line) simulations. Month 1 is January. (a) Land areas from 60–90° N. (b) Ocean areas from 60–90° N.

climate in southern Mexico and west Africa (Somalia). Subtropical (Cfa) climates replace marine climates (Cfb, Cfc) in North America and Europe because of warmer summer temperatures. Marine climates migrate poleward and replace cool-temperate (D) climates in Europe, North America, and New Zealand, while cool-temperate climates migrate poleward and replace tundra (ET) climates in the Arctic and Antarctic. Lowland tundra is greatly restricted in areal extent and occupies just a few grid cells along the fringes of the Arctic Ocean.

5. COMPARISON OF SIMULATIONS AND PALAEOCLIMATIC INDICATORS

Comparison of the BARESOIL and BESTGUESS simulations with the global distribution of palaeoclimatic indicators demonstrates that inclusion of forest vegetation improves correspondence between simulated and actual palaeoclimate. The BARESOIL simulation (figure 10a) incorrectly predicts tundra (ET) climates for large regions of Alaska, Siberia, and coastal Antarctica, regions where fossil assemblages indicate forests (and hence warm-month means higher than 10 °C). The areal distribution of tropical rainforest is also underestimated relative to proxy data, especially for Africa. In contrast, the BESTGUESS simulation (figure 10b) shows a much better fit, with indicators of forest vegetation. Forest vegetation is correctly predicted for Siberia, Alaska, and the southern Antarctic Peninsula, in contrast to BARESOIL. This improved correspondence between model output and indicators of forest vegetation indicates that the presence of trees causes warm-month means to exceed 10 °C and creates the conditions needed for the persistence of forest vegetation. Tropical rainforest sites are better predicted by the BESTGUESS simulation than by the BARESOIL simulation, a result that parallels model simulations for the Recent tropics (Dickinson & Henderson-Sellers 1988; Shukla *et al.* 1990). For the Recent tropics, replacement of tropical rainforest by grasslands creates hotter and drier

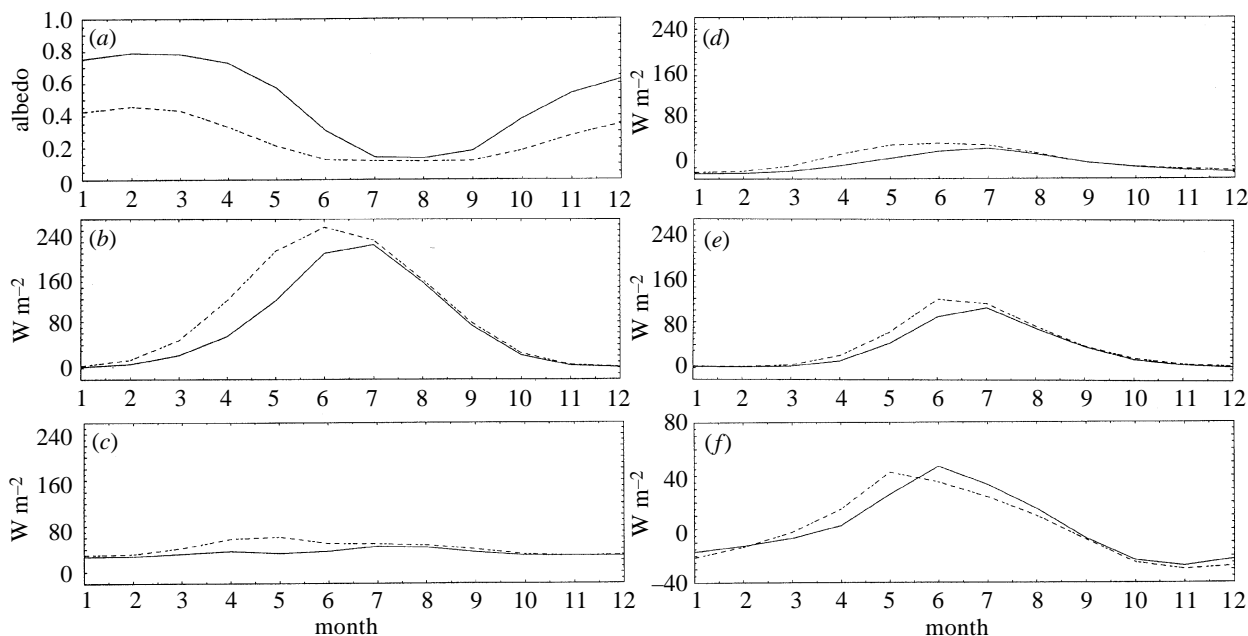


Figure 9. Annual cycle of the surface energy budget for land areas 60–90° N, BESTGUESS (dashed lines) and BARESOIL (solid lines) simulations. (a) Surface albedo, (b) surface absorbed solar radiation ( $\text{W m}^{-2}$ ), (c) net surface infrared radiation ( $\text{W m}^{-2}$ ), (d) surface sensible heat flux ( $\text{W m}^{-2}$ ), (e) surface latent heat flux ( $\text{W m}^{-2}$ ), (f) net surface heat flux ( $\text{W m}^{-2}$ ).

conditions. These results mean that the presence of trees in equatorial regions can help to create the climatic conditions that favour the persistence of tropical rainforests.

Greater discrepancies exist between model simulations and proxy data for middle latitudes. Simulated climates for latitudes between 35° and 55° are too cool to support the warm-temperate to subtropical broad-leaved vegetation prescribed in the BESTGUESS run. Palaeobotanical indicators of above-freezing winter temperatures conflict with predicted cold-month means in continental interiors at high middle latitudes (figure 11). Cold-month means of 5 °C and 1 °C, which predict the occurrence of biologically significant freezing on a global scale (Prentice *et al.* 1992) and in East Asia (Wolfe 1979), respectively, occur as much as 15° south of above-freezing indicators in all simulations in the Northern Hemisphere. Indicators of above-freezing winters are diverse, and include palms and gingers which cannot tolerate below-freezing cold-month means and prolonged exposure to hard freezes (Box 1981; Wing & Greenwood 1993). Also indicative of above-freezing conditions are Greenland leaf assemblages with inferred mean annual temperatures greater than 20 °C (lower Atanikerdruk leaf assemblages) (Wolfe & Upchurch 1987). Modern climates with mean annual temperatures greater than 20 °C always have cold-month means that are well-above freezing (Wolfe 1979, plate 2).

## 6. DISCUSSION

Our simulations indicate that forest vegetation played an important role in maintaining high-latitude warmth during the Late Cretaceous, and underscore the importance of vegetation as an active agent of global climate change. The presence of high-latitude deciduous forests significantly decreases albedo and significantly increases fluxes between the land surface and the atmosphere.

Changes in albedo are greater than changes in surface fluxes, and result in a net warming of the land surface. Warming occurs year-round but is most pronounced in late spring and summer during maximal solar insolation. This causes an increase in summer temperatures and a lengthening of the growing season to a point at which the local climate is favourable to forest vegetation.

Previous authors have suggested that vegetation has properties that alter climate and ensure its persistence on the landscape. In a study of the grassland–forest boundary, Woodcock (1992) suggested that grassland vegetation helps to maintain dry conditions and a propensity to burning through its relatively high albedo, low LAI, and high production of leaf litter. This reduces rainfall through reduced evapotranspiration and reduced absorption of solar radiation and creates conditions favourable to the ignition of fires. Forest vegetation, in contrast, helps to maintain wetter conditions and a lower propensity to burning through its low albedo, high LAI, and low production of leaf litter relative to stem material. This increases rainfall through increased evapotranspiration and increased absorption of solar radiation, and creates conditions less favourable to the ignition of fires. Bonan *et al.* (1995) compared the climatic effects of evergreen boreal coniferous forest and tundra vegetation. Their results indicate that evergreen boreal conifer forests create feedbacks with the climate that regulate surface temperature and help create the climatic conditions necessary for their existence.

Our simulations provide additional evidence that albedo, LAI, and other attributes of forest vegetation help to create the climatic conditions that favour the persistence of forests on the landscape. At high latitudes, this property of forest vegetation is markedly illustrated by a comparison of the BARESOIL and BESTGUESS simulations. Here, the presence of temperate deciduous forests

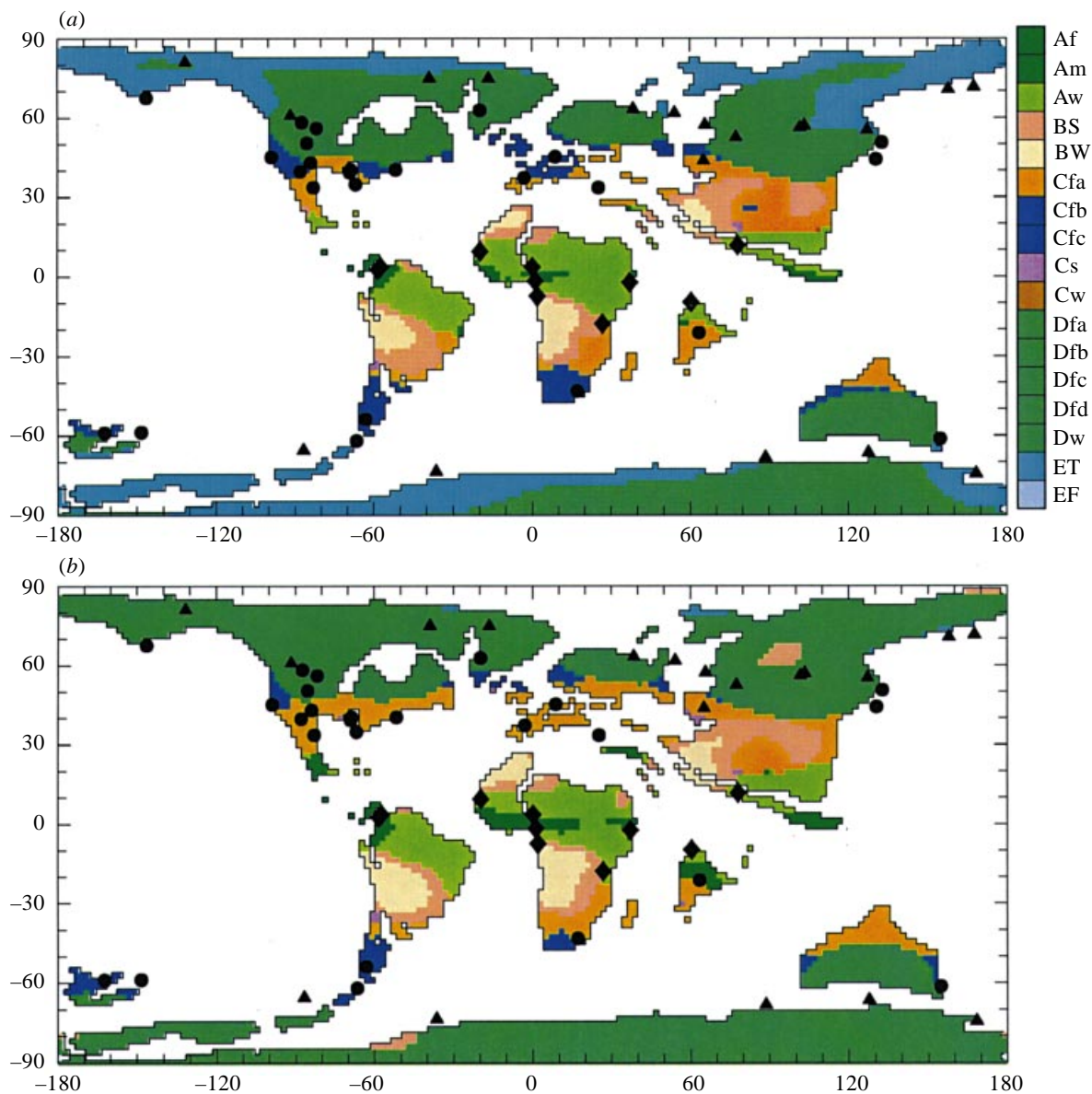


Figure 10. Predicted climates and the distribution of forest/woodland vegetation under (a) BARESOIL and (b) BESTGUESS simulations. Climates correspond to the modified Köppen scheme described in the text (Köppen 1936). The humid-subhumid boundary has been altered to account for overestimation of precipitation in GENESIS v. 1.02. Tundra (ET) and boreal (D) forests are separated by a warm-month mean temperature of 10 °C; subtropical (Cfa) and marine (Cfb, Cfc) climates are separated by a 1-month mean temperature of 20 °C; warm-temperate (C) and cool-temperate (D) climates are separated by a cold-month mean temperature of 1 °C. The basis for inferring forest and woodland vegetation is explained in the text. Diamonds, tropical forest; circles, subtropical forest; triangles, cool-temperate (deciduous) forest.

There is an increase in summer temperatures, and a lengthening of the growing season beyond the threshold needed for tree growth. Late Cretaceous deciduous forests of high latitudes, like Recent evergreen boreal forests, helped ensure their own persistence on the landscape because of their low albedoes resulting from high LAI, high fractional cover, and masking of snow cover. Data on vegetation cover for the latest Cretaceous are sparse, but our simulations indicate that individual tropical forest types also may have altered regional climate in a manner favourable to their own persistence. Tropical rainforest vegetation shows a greater areal extent in the BESTGUESS simulation than in the BARESOIL simulation. Regions of tropical deciduous vegetation show change in areal distribution between simulations, but

have surface temperatures that are as much as 4 °C higher in the BESTGUESS simulation relative to the BARESOIL simulation. This increase in surface temperature results from a decrease in albedo, which causes a corresponding increase in absorbed solar radiation. Increased heating of the land surface in the absence of compensatory changes increases drought stress on vegetation, which decreases the adaptive advantage of tropical rainforest life forms relative to those of drier and hotter climates (Box 1981). Our model simulations demonstrate important climatic linkages between the land surface, atmosphere, and oceans at high latitudes. These indicate that forest vegetation may be an important factor in maintaining ice-free conditions at high latitudes, a critical factor in maintaining warm polar temperatures during geologic intervals such as the

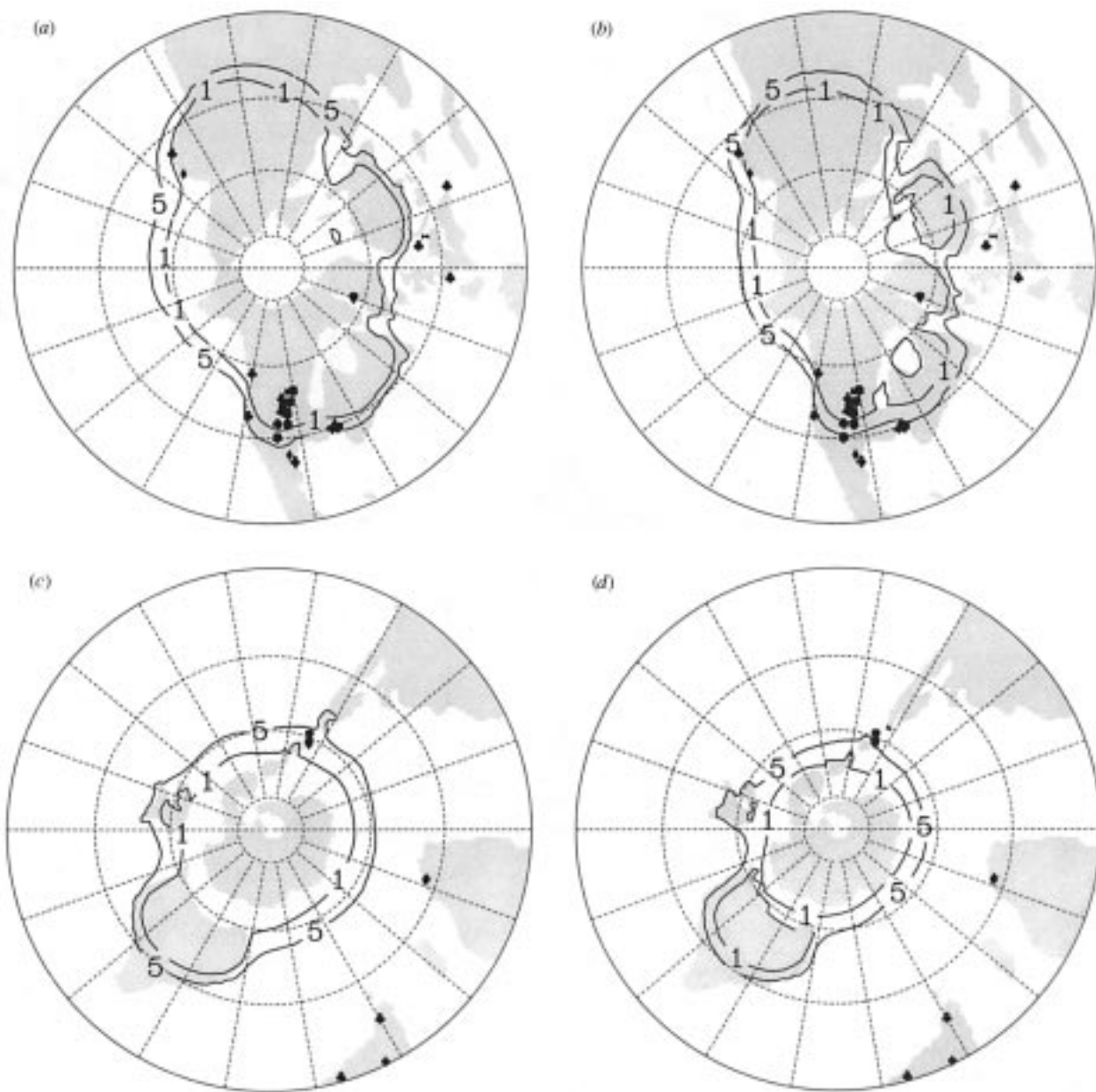


Figure 11. Predicted distribution of 1 °C and 5 °C cold-month means and the distribution of above-freezing palaeobotanical indicators, Northern and Southern Hemispheres. (a) BARESOIL, Northern Hemisphere (January), (b) BESTGUESS, Northern Hemisphere (January), (c) BARESOIL, Southern Hemisphere (July), (d) BESTGUESS, Northern Hemisphere (July). Note how the above-freezing indicators extend poleward of the simulated isotherms in the Western Interior of North America and in Greenland.

Cretaceous (Rind & Chandler 1991). High-latitude forests, with their low surface albedo relative to bare soil, warm adjacent oceans by as much as 12 °C. The first steps in this process are (1) increasing land surface temperatures; (2) transferring heat from the land surface to the atmosphere; and then (3) transferring heat from the atmosphere to the oceans. The extra heat transferred from the atmosphere to the oceans initiates a series of positive feedbacks that result in additional warming. Ocean warming causes a delay in the formation of sea-ice in winter and a reduction in its thickness and fractional cover. This causes sea-ice to melt faster and earlier in the spring because of its reduced thickness and fractional cover. Earlier melting of sea-ice allows greater ocean warming during the spring and summer, which further inhibits sea-ice development during the

autumn and winter. Inhibition of sea-ice development lowers the average albedo of the ocean and causes the ocean to absorb more solar radiation.

## 7. CONCLUSIONS

High-latitude deciduous forests played an important role in maintaining polar warmth during the latest Cretaceous. The presence of high-latitude deciduous forests in model simulations warms temperatures relative to bare soil conditions and creates the necessary warmth for the persistence of trees rather than tundra herbs. This warming occurs by a decrease in albedo of forest vegetation relative to bare soil, and a corresponding increase in absorbed solar radiation. Much of the extra energy

erbed by the land surface is transferred to adjacent oceans, which initiates a series of positive feedbacks that warm the oceans and land climate. The combined success and failure of our climate simulations in recreating latest Cretaceous terrestrial climate suggests that several mechanisms probably acted in concert to create the warm conditions of the Late Cretaceous and other periods of high global temperature. Increased atmospheric pCO<sub>2</sub> increased absorption of infrared radiation, both directly and through its effect on atmospheric water vapour, a potent greenhouse gas. Widely extensive polar forests increased absorption of solar radiation at high latitudes and warmed temperatures around the world. Increased ocean (and atmospheric?) heat transport may have increased high-latitude winter temperatures while simultaneously preventing the tropics from overheating under strong greenhouse forcing. Positive feedbacks between the land, ocean, and atmosphere may have increased high-latitude temperatures. A multi-mechanism model with positive feedbacks is intuitively appealing and explains many seemingly unrelated climatic conditions for the Late Cretaceous. However, the ultimate validity of this hypothesis will be determined by future modelling studies performed in conjunction with more stringent comparisons of model output and the paleoclimatic record.

Thank S. Thompson and D. Pollard for providing us with the ESM climate model, and E. Becker and T. Morgan for assistance with graphics. Research was supported by the Texas Higher Education Coordinating Board Advanced Research Program, grant 3615-029, and by a Southwest Texas State University Research Enhancement Grant. Computer simulations were performed at the University of Texas Center for High-Performance Computing and the National Center for Atmospheric Research, which is supported by the US National Science Foundation.

## REFERENCES

Andrews, J. E., Tandon, S. K. & Dennis, D. F. 1995 Concentration of carbon dioxide in the Late Cretaceous atmosphere. *J. Geol. Soc. Lond.* **152**, 1–3.

Bray, I. W. & Sinnott, E. W. 1916 The climatic distribution of certain types of angiosperm leaves. *Am. J. Bot.* **3**, 24–39.

Condon, E. J. & Washington, W. M. 1982 Cretaceous climate: a comparison of atmospheric simulations with the geologic record. *Palaeo. Palaeo. Palaeo.* **40**, 103–133.

Condon, E. J. & Washington, W. M. 1985 Warm Cretaceous climates: high atmospheric CO<sub>2</sub> as a plausible mechanism. In *The carbon cycle and atmospheric CO<sub>2</sub>: natural variations, Archean to present* (ed. E. T. Sundquist & W. S. Broecker), pp. 546–553. Philosophical Monographs Series. Washington, DC: American Philosophical Union.

Bryson, R. A. 1991 A model for atmospheric CO<sub>2</sub> over the Phanerozoic time. *Am. J. Sci.* **291**, 339–376.

Bryson, R. A. 1994 Geocarb II: a revised model of atmospheric CO<sub>2</sub> over Phanerozoic time. *Am. J. Sci.* **294**, 56–91.

Condon, E. J., Pollard, D. & Thompson, S. L. 1992 Effects of realistic forest vegetation on global climate. *Nature* **359**, 715–718.

Condon, E. J., Chapin, F. S. III & Thompson, S. L. 1995 Boreal forest and tundra ecosystems as components of the climate system. *Clim. Change* **29**, 145–167.

Condon, E. O. 1981 *Macrocclimate and plant forms: an introduction to predictive modeling in phytogeography*. The Hague: Dr W. Junk Publishers.

Brass, G. W., Southam, J. R. & Peterson, W. H. 1982 Warm saline bottom water in the ancient ocean. *Nature* **296**, 620–623.

Bryson, R. A. 1966 Air masses, streamlines, and the boreal forest. *Geogr. Bull.* **8**, 228–269.

Cerling, T. E. 1991 Carbon dioxide in the atmosphere: evidence from Cenozoic and Mesozoic paleosols. *Am. J. Sci.* **291**, 377–400.

Cerling, T. E., Quade, J. & Wang, Y. 1994 Expansion and emergence of C<sub>4</sub> plants. *Nature* **371**, 112–113.

Covey, C. & Thompson, S. L. 1989 Testing the effects of ocean heat transport on climate. *Palaeo. Palaeo. Palaeo.* **75**, 331–341.

Creber, G. T. & Chaloner, W. G. 1985 Tree growth in the Mesozoic and Early Tertiary and the reconstruction of palaeoclimates. *Palaeo. Palaeo. Palaeo.* **52**, 35–60.

Crepet, W. L. & Feldman, G. D. 1991 The earliest remains of grasses in the fossil record. *Am. J. Bot.* **78**, 1010–1014.

Crowley, T. J. 1991 Past CO<sub>2</sub> changes and tropical sea surface temperatures. *Paleoceanography* **6**, 387–394.

Crowley, T. J. & Baum, S. K. 1992 Modeling late Paleozoic glaciation. *Geology* **20**, 507–510.

Dickinson, R. E. & Henderson-Sellers, A. 1988 Modelling tropical deforestation: a study of GCM land-surface parameterizations. *Q. J. R. Met. Soc.* **114**, 439–462.

Dickinson, R. E., Henderson-Sellers, A., Kennedy, P. J. & Wilson, M. F. 1986 Biosphere-Atmosphere Transfer Scheme (BATS) for the NCAR Community Climate Model. *NCAR Technical Note* TN-275+STR, 1–69.

Dilcher, D. L. 1965 Epiphyllous fungi from the Eocene deposits in western Tennessee, USA. *Palaeontographica Abt. B* **116**, 1–54.

Dorman, J. L. & Sellers, P. J. 1989 A global climatology of albedo, roughness length and stomatal resistance for atmospheric general circulation models as represented by the Simple Biosphere Model (SiB). *J. Appl. Met.* **28**, 833–855.

Endal, A. S. 1981 Evolutionary variations of solar luminosity. Variations of the Solar Constant. *NASA Conf. Publ.* **2191**, 175–183.

Foley, J. A., Kutzbach, J. E., Coe, M. T. & Levis, S. 1994 Feedbacks between climate and boreal forests during the Holocene epoch. *Nature* **371**, 52–53.

Freeman, K. H. & Hayes, J. M. 1992 Fractionation of carbon isotopes by phytoplankton and estimates of ancient CO<sub>2</sub> levels. *Global Biogeochem. Cycles* **6**, 185–198.

Hay, W. W. 1984 The breakup of Pangaea: climatic, erosional and sedimentological effects. *Proceedings of the 27th International Geological Congress*, Section 6, pp. 15–38.

Horrell, M. A. 1991 Phytogeography and paleoclimatic interpretation of the Maestrichtian. *Palaeo. Palaeo. Palaeo.* **86**, 87–138.

Huber, B. T., Hodell, D. A. & Hamilton, C. P. 1995 Middle-Late Cretaceous climate of the southern high latitudes: stable isotopic evidence for minimal equator-to-pole thermal gradients. *Geol. Soc. Am. Bull.* **107**, 1164–1191.

Köppen, W. 1936 Das Geographische System der Klimate. In *Handbuch der Klimatologie* (ed. W. Köppen & R. Geiger), pp. C-1–C-44. Berlin: Gebrüder Borntraeger.

Muller, J. 1981 Fossil pollen records of extant angiosperms. *Bot. Rev. (Lancaster)* **47**, 1–142.

Otto-Bliesner, B. L. & Upchurch, G. R. Jr 1997 Vegetation-induced warming of high latitude regions during the Late Cretaceous period. *Nature* **385**, 804–807.

Pielke, R. A. & Vidale, P. L. 1995 The boreal forest and the polar front. *J. Geophys. Res.* **100** (D12), 25, 755–758.

Pollard, D. & Thompson, S. L. 1995 Use of a land-surface-transfer scheme (LSX) in a global climate model: the response to doubling stomatal resistance. *Global Planetary Change* **10**, 129–161.

Prentice, I. C., Cramer, W., Harrison, S. P., Leemans, R., Monserud, R. A. & Solomon, A. M. 1992 A global biome

- model based on plant physiology and dominance, soil properties, and climate. *J. Biogeogr.* **19**, 117–134.
- Rind, D. & Chandler, M. 1991 Increased ocean heat transports and warmer climate. *J. Geophys. Res.* **96**, 7437–7461.
- Schneider, S. H., Thompson, S. L. & Barron, E. J. 1985 Mid-Cretaceous continental surface temperatures: are high CO<sub>2</sub> concentrations needed to simulate above-freezing conditions? In *The carbon cycle and atmospheric CO<sub>2</sub>: natural variations, Archean to present* (ed. E. T. Sundquist & W. S. Broecker), pp. 554–560. Geophysical Monographs Series. Washington, DC: American Geophysical Union.
- Sellers, P. J. & Dorman, J. L. 1987 Testing the Simple Biosphere Model (SiB) using point micrometeorological and biophysical data. *J. Clim. Appl. Met.* **26**, 622–651.
- Sellers, P. J., Mintz, Y., Sud, Y. C. & Dalcher, A. 1986 A Simple Biosphere (SiB) Model for use within general circulation models. *J. Atmos. Sci.* **43**, 505–531.
- Semter, A. J. Jr 1976 A model for the thermodynamic growth of sea-ice in numerical investigations of climate. *J. Phys. Oceanogr.* **6**, 379–389.
- Shukla, J., Nobre, C. & Sellers, P. 1990 Amazon deforestation and climate change. *Science* **247**, 1322–1325.
- Sloan, L. C. & Barron, E. J. 1990 'Equable' climates during Earth history? *Geology* **18**, 489–492.
- Sloan, L. C. & Barron, E. J. 1992 A comparison of Eocene climate model results to quantified paleoclimatic interpretations. *Palaeo. Palaeo. Palaeo.* **93**, 183–202.
- Spicer, R. A. & Parrish, J. T. 1990 Late Cretaceous–Early Tertiary palaeoclimates of northern high latitudes: a quantitative view. *J. Geol. Soc. Lond.* **147**, 329–341.
- Thompson, S. L. & Pollard, D. 1995a A global climate model (GENESIS) with a land-surface transfer scheme (LSX). I. Present climate simulation. *J. Clim.* **8**, 732–761.
- Thompson, S. L. & Pollard, D. 1995b A global climate model (GENESIS) with a land-surface transfer scheme (LSX). II. CO<sub>2</sub> sensitivity. *J. Clim.* **8**, 1104–1121.
- Upchurch, G. R. Jr 1995 Dispersed angiosperm cuticles: their history, preparation, and application to the rise of angiosperms in Cretaceous and Paleocene coals, southern Western Interior of North America. *Int. J. Coal Geol.* **28**, 161–227.
- Upchurch, G. R. Jr & Wolfe, J. A. 1993 Cretaceous vegetation of the Western Interior and adjacent regions of North America. In *Evolution of the Western Interior Basin* (ed. W. G. E. Caldwell & E. G. Kauffman), pp. 243–281. Geological Society of Canada Special Paper no. 39.
- Upchurch, G. R. Jr, Otto-Bliessner, B. L. & Scotese, C. 1998 Terrestrial vegetation and its effects on climate during the Late Cretaceous. In *The evolution of Cretaceous ocean/climate systems*. Geological Society of America Special Paper Series (ed. E. Barrera & C. C. Johnson). Boulder, CO: Geological Society of America.
- Wing, S. L. & Greenwood, D. R. 1993 Fossils and fossil climate: the case for equable continental interiors in the Eocene. *Phil. Trans. R. Soc. Lond. B* **341**, 243–252.
- Wing, S. L., Hickey, L. J. & Swisher, C. C. 1993 Implications of an exceptional fossil flora for Late Cretaceous vegetation. *Nature* **363**, 342–344.
- Wolfe, J. A. 1979 Temperature parameters of humid to mesic forests of eastern Asia and their relation to forests of other regions of the Northern Hemisphere and Australasia. *US Geol. Surv. Profess. Paper* **1106**, 137.
- Wolfe, J. A. 1994 Alaskan Palaeogene climates as inferred from the Clamp database. *NATO ASI Series* **127**, 223–237.
- Wolfe, J. A. & Upchurch, G. R. Jr 1987 North American non-marine climates and vegetation during the Late Cretaceous. *Palaeo. Palaeo. Palaeo.* **61**, 33–77.
- Woodcock, D. W. 1992 The rain on the plain: are there vegetation-climate feedbacks? *Palaeo. Palaeo. Palaeo.* **97**, 191–201.
- Ziegler, A. M., Raymond, A. L., Gierlowski, T. C., Horrell, M. A., Rowley, D. B. & Lottes, A. L. 1987 Coal, climate, and terrestrial productivity: the present and early Cretaceous compared. In *Coal and coal-bearing strata: recent advances* (ed. A. C. Scott), pp. 25–49. Geological Society Special Publication. London: Geological Society of London.
- Ziegler, A. M., Rowley, D. B., Lottes, A. L., Sahagian, D. L., Hulver, M. L. & Gierlowski, T. C. 1985 Palaeogeographic interpretation: with an example from the mid-Cretaceous. *A. Rev. Earth Planet. Sci.* **13**, 385–425.

### Discussion

T. LENTON (*School of Environmental Sciences, University of East Anglia, Norwich, UK*). Could part of the reason that your model gives high-latitude winter temperatures that are too cold be that you cannot iterate the warming effect of forest, which might cause it to spread further?

G. UPCHURCH. Our simulation of winter temperatures is too cold for at least three reasons. First, our BESTGUESS simulation prescribes winter-deciduous trees for the Arctic and much of the Antarctic. This prescription is based on extensive palaeobotanical evidence for widespread polar deciduous forest during the Late Cretaceous. Prescribing a vegetation of dense evergreen trees, as we did in our EVERGREEN TREE simulation, increases winter warming because the snow blows off green leaves in the canopy. The exposed green leaves effectively mask the snow, which decreases albedo and increases absorbed solar radiation. Polar deciduous forests have no leaves during the winter, so winter albedo in BESTGUESS is higher than that in EVERGREEN TREE because bare stems provide less masking of snow cover.

Second, even with a prescribed vegetation of evergreen trees our model cannot transport sufficient heat to the poles to explain the record of winter-temperature proxies, especially cold-sensitive plants at high middle latitudes. This could result from inadequacies in the GENESIS atmospheric model. Alternatively, it could result in our underestimating ocean heat transport, which is prescribed at modern-day values in four of our five simulations. Increasing ocean heat transport increases high-latitude warming beyond the effects of vegetation. The importance of increased ocean-heat transport is currently unclear because ocean modellers do not yet agree on whether Cretaceous oceans actually transported greater amounts of heat than Recent oceans and, if so, exactly how.

Finally, we could have prescribed levels of atmospheric pCO<sub>2</sub> in our simulations that were much lower than the actual values for the latest Cretaceous. Our prescribed levels (580 ppm) are higher than Bob Berner's best estimate from geochemical modelling but are significantly lower than estimates from isotopic proxies, which place the value as high as 1400–1500 ppm.

P. VALDES (*Department of Meteorology, University of Reading, UK*). Much of the data on warm winters is for coastal sites, especially for those regions where the 'all soil' model differs from the 'realistic vegetation' model. What is the importance of ocean heat transport?

G. UPCHURCH. Enhanced ocean heat transport, if it existed during the Late Cretaceous, would help solve the problem of winter warmth at high latitudes, especially for coastal regions where most of the temperature proxies are located.



in opinion, however, proponents of enhanced ocean heat transport have yet to prove their case. Stronger surface winds on the ocean, one possible mechanism of enhancing heat transport, are not likely based on the wind fields in our simulations. Generation of warm saline bottom water, the commonly proposed mechanism for enhancing ocean heat transport and creating warm polar oceans, is plausible but has yet to be demonstrated conclusively through either the geologic record of isotopic proxies or ocean general circulation models (OGCM's). Physically, making warm water sink is much more difficult than making cold water sink even if the warm water is saline.

**BEERLING** (*Department of Animal and Plant Sciences, University of Sheffield, UK*). If I understand your modelling correctly, you have assigned fixed values of leaf area index (LAI) and stomatal conductance ( $g_s$ ) to each type of vegetation based on those of the closest modern analogues. In practice, however, the LAI and stomatal resistance varies even within a given vegetation type, will be strongly dependent on climate (leaf-to-air vapour pressure deficit, temperature, precipitation regime), and particularly on the concentration of atmospheric  $CO_2$ . Have you investigated the sensitivity of the magnitude of vegetation feedbacks on climate to variations in LAI and  $g_s$ ?

**UPCHURCH**. I will first explain the two terms for the general reader, then answer the question. LAI measures the number of leaf layers in the canopy. Rain forest vegetation has high LAI (typically 5–6) while desert vegetation has low LAI (typically 1 or less). Stomatal conductance ( $g_s$ ) is the rate at which  $CO_2$  diffuses into the leaf and water vapour diffuses out. Stomatal conductance is determined by the size and number of stomata (gas-exchange pores), the extent to which the stomata open, available soil moisture and the vapour-pressure deficit between the leaf and atmosphere.

LAI in the GENESIS model is prescribed; in our paleoclimate simulations we make it vary with the modern if such variation occurs in the modern analogue vegetation. We investigated LAI and its effects on climate in three simulations: (1) BARESOIL (LAI=0, or no leaves whatsoever for the entire land surface), (2) EVERGREEN TREE (LAI=6, or the dense leaves of rain forest vegetation for the entire land surface), and (3) BESTGUESS (LAI varies with vegetation types, which ranges from desert to tropical rain forest). Finer-scale studies, in

which LAI varies over the geographic range of a single vegetation type, were not conducted.

Increasing LAI decreases surface albedo while simultaneously increasing surface roughness and the flux of water vapour to the atmosphere. These effects are of opposite sign and feed back into such atmospheric processes as cloud formation to determine the radiation budget of the land surface.

Two comparisons illustrate the effects of LAI on surface warming. First, comparison of our EVERGREEN TREE simulation (maximum leaf area over the land surface) with our BARESOIL simulation (no leaves), indicates that an increased LAI can cause surface warming. Global temperatures are 2.5 °C higher in EVERGREEN TREE because the decrease in surface albedo causes an increase in absorbed solar radiation. This warming affects most regions of the world.

Comparison of our EVERGREEN TREE simulation with our BESTGUESS simulation indicates that high LAI can have a cooling effect relative to moderate LAI (LAI=2–4, or the leaf area typical of a deciduous forest in the spring and summer). High LAI increases evaporative cooling and the flux of water vapour to the atmosphere relative to moderate LAI. This, in turn, can cause an increase in clouds, which reflect more of the incoming solar radiation and cause the land surface to absorb less energy. In our simulations this cooling under high LAI is especially pronounced in two regions: (1) tropical regions that support dry-season deciduous vegetation, and (2) high-latitude regions that support forest vegetation.

Stomatal conductance ( $g_s$ ) in GENESIS is based on a prescribed maximum conductance and physiological response functions for light and temperature taken from the closest modern analogue vegetation. Transpiration is determined by these functions in combination with the values for light, temperature, and soil moisture at the land surface. To approximate the effects of elevated atmospheric  $pCO_2$  on stomatal conductance we halved the maximum conductance for all vegetation types. The major effect we observed in our simulations was a slight increase in sensible heating of the land surface, which was statistically significant only over limited regions.

These results are described and illustrated more fully in Upchurch *et al.* (1998).